J|A|C|S
ARTICLES
Published on Web 04/05/2003

Modeling the Stereoselectivity of the β-Amino Alcohol-Promoted Addition of Dialkylzinc to Aldehydes

Torben Rasmussen[†] and Per-Ola Norrby*[,‡]

Contribution from the Department of Medicinal Chemistry, Royal Danish School of Pharmacy, Universitetsparken 2, DK-2100 Copenhagen, Denmark, and Department of Chemistry, Technical University of Denmark, Building 201, Kemitorvet, DK-2800 Kgs. Lyngby, Denmark

Received November 11, 2002; E-mail: pon@kemi.dtu.dk

Abstract: The title reaction has been modeled by a Q2MM force field, allowing for rapid evaluation of several thousand TS conformations. For 10 experimental systems taken from the literature, the pathway leading to the major enantiomer has been identified. Furthermore, several possible contributions to the minor enantiomer have been investigated, providing an identification of the reasons for the sometimes moderate enantioselectivity of the title reaction, and allowing for future rational improvement of existing ligands. The favored pathways to the minor enantiomer, which must be blocked for significant selectivity improvement, differ strongly among ligands. Thus, design ideas are not necessarily transferable between ligand classes, but must be developed for each reaction on the basis of the pathway that needs to be blocked in each specific case. However, we have identified some general structure−selectivity relationships.

Introduction

One of the holy grails in modern organic synthesis is to build chiral organic molecules in a highly selective manner. An important class of reactions for constructing carbon−carbon bonds with the potential for stereocontrol is the addition of carbon nucleophiles to carbonyl compounds, for example, the classical Grignard reaction. It has generally been found that stereocontrol is most easily achieved by selective promotion or catalysis of comparably unreactive systems, where the racemic background reaction is slow. A number of elegant investigations in the 1980s established the broad utility of enantioselective addition of dialkylzinc to aldehydes (Scheme 1).[1,2] Since then, an overwhelming number of greatly varied ligands have been shown to promote this reaction in an enantioselective way, making the reaction increasingly useful in synthetic chemistry.

Scheme 1. Ligand Promoted Asymmetric Addition of Dialkylzinc to Aldehydes

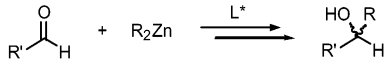

Some recent examples are listed in the references.[3] The most common test case has been addition of diethylzinc to benzaldehyde, mainly due to the low availability of other zinc reagents, but the scope of the reaction has recently taken a leap with the application of diarylzinc reagents, leading to diaryl methanols.[4] Such products are extremely hard to form in a stereoselective manner by other methods. It has also been shown that the reaction can be catalyzed by chiral Lewis acids, especially Ti-based complexes.[2c,d]

Noyori and co-workers have studied the mechanism of the title reaction extensively using both theoretical[5] and experi-

[†] Royal Danish School of Pharmacy. Current address: Department of Theoretical Chemistry, Lund University, Chemical Center, P.O. Box 124, SE-221 00 Lund, Sweden.

[‡] Technical University of Denmark.

(1) (a) Sato, T.; Soai, K.; Suzuki, K.; Mukaiyama, T. *Chem. Lett.* **1978**, 601−604. (b) Mukaiyama, T.; Soai, K.; Sato, T.; Shimizu, H.; Suzuki, K. *J. Am. Chem. Soc.* **1979**, *101*, 1455−1460. (c) Oguni, N.; Omi, T.; Yamamoto, Y.; Nakamura, A. *Chem. Lett.* **1983**, 841−842. (d) Oguni, N.; Omi, T. *Tetrahedron Lett.* **1984**, *25*, 2823−2824. (e) Kitamura, M.; Suga, S.; Kawai, K.; Noyori, R. *J. Am. Chem. Soc.* **1986**, *108*, 6071−6072. (f) Itsuno, S.; Fréchet, J. M. J. *J. Org. Chem.* **1987**, *52*, 4140−4142. (g) Soai, K.; Yokoyama, S.; Ebihara, K.; Hayasaka, T. *J. Chem. Soc., Chem. Commun.* **1987**, 1690−1691. (h) Soai, K.; Ookawa, A.; Kaba, T.; Ogawa, K. *J. Am. Chem. Soc.* **1987**, *109*, 7111−7115. (i) Soai, K.; Ookawa, A.; Ogawa, K.; Kaba, T. *J. Chem. Soc., Chem. Commun.* **1987**, 467−468. (j) Smaardijk, A. A.; Wynberg, H. *J. Org. Chem.* **1987**, *52*, 135−137. (k) Chaloner, P. A.; Perera, S. A. R. *Tetrahedron Lett.* **1987**, *28*, 3013−3014. (l) Oguni, N.; Matsuda, Y.; Kaneko, T. *J. Am. Chem. Soc.* **1988**, *110*, 7877−7878. (m) Kitamura, M.; Okada, S.; Suga, S.; Noyori, R. *J. Am. Chem. Soc.* **1989**, *111*, 4028−4036. (n) Corey, E. J.; Yuen, P.-W.; Hannon, F. J.; Wierda, D. A. *J. Org. Chem.* **1990**, *55*, 784−786.

(2) For reviews see: (a) Evans, D. A. *Science* **1988**, *240*, 420−426. (b) Noyori, R.; Kitamura, M. *Angew. Chem., Int. Ed. Engl.* **1991**, *30*, 49−69. (c) Soai, K.; Niwa, S. *Chem. Rev.* **1992**, *92*, 833−856. (d) Pu, L.; Yu, H.-B. *Chem. Rev.* **2001**, *101*, 757−824.

(3) (a) Tanner, D.; Kornø, H. T.; Guijarro, D.; Andersson, P. G. *Tetrahedron* **1998**, *54*, 14213−14232. (b) Cho, B. T.; Chun, Y. S. *Tetrahedron: Asymmetry* **1998**, *9*, 1489−1492. (c) Solà, L.; Reddy, K. S.; Vidal-Ferran, A.; Moyano, A.; Pericàs, M. A.; Riera, A.; Alvarez-Larena, A.; Piniella, J.-F. *J. Org. Chem.* **1998**, *63*, 7078−7082. (d) Guijarro, D.; Pinho, P.; Andersson, P. G. *J. Org. Chem.* **1998**, *63*, 2530−2535. (e) Shi, M.; Satoh, Y.; Masaki, Y. *J. Chem. Soc., Perkin Trans. 1* **1998**, 2547−2552. (f) Yang, X.; Shen, J.; Da, C.; Wang, R.; Choi, M. C. K.; Yang, L.; Wong, K. *Tetrahedron: Asymmetry* **1999**, *10*, 133−138. (g) Wassmann, S.; Wilken, J.; Martens, J. *Tetrahedron: Asymmetry* **1999**, *10*, 4437−4445. (h) Sibi, M. P.; Chen, J.-X.; Cook, G. R. *Tetrahedron Lett.* **1999**, *40*, 3301−3304. (i) Lawrence, C. F.; Nayak, S. K.; Thijs, L.; Zwanenburg, B. *Synlett* **1999**, *10*, 1571−1572. (j) Kossenjans, M.; Soeberdt, M.; Wallbaum, S.; Harms, K.; Martens, J.; Aurich, H. G. *J. Chem. Soc., Perkin Trans. 1* **1999**, 2353−2365. (k) Paleo, M. R.; Cabeza, I.; Sardina, F. J. *J. Org. Chem.* **2000**, *65*, 2108−2113. (l) Reddy, K. S.; Solà, L.; Moyano, A.; Pericàs, M. A.; Riera, A. *Synthesis* **2000**, *1*, 165−176. (m) Kawanami, Y.; Mitsuie, T.; Miki, M.; Sakamoto, T.; Nishitani, K. *Tetrahedron* **2000**, *56*, 175−178. (n) Dai, W.-M.; Zhu, H.-J.; Hao, X.-J. *Tetrahedron: Asymmetry* **2000**, *11*, 2315−2337. (o) Ooi, T.; Saito, A.; Maruoka, K. *Chem. Lett.* **2001**, 1108−1109. (p) Hu, Q.-S.; Sun, C.; Monaghan, C. E. *Tetrahedron Lett.* **2001**, *42*, 7725−7728. (q) Ohga, T.; Umeda, S.; Kawanami, Y. *Tetrahedron* **2001**, *57*, 4825−4829. (r) Steiner, D.; Sethofer, S. G.; Goralski, C. T.; Singaram, B. *Tetrahedron: Asymmetry* **2002**, *13*, 1477−1483. (s) Xu, Q.; Zhu, G.; Pan, X.; Chan, A. S. C. *Chirality* **2002**, *14*, 716−723. (t) Sato, I.; Kodaka, R.; Hosoi, K.; Soai, K. *Tetrahedron: Asymmetry* **2002**, *13*, 805−808.

10.1021/ja0292952 CCC: $25.00

Scheme 2. Catalytic Cycle for β-Amino Alcohol Promoted Addition of Dialkylzinc to Aldehydes

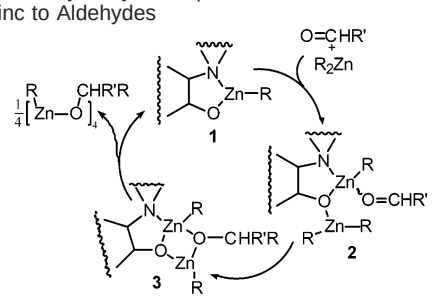

mental[1m,2b,6] methods. The true asymmetric catalyst is believed to be a zinc alkoxide where the nitrogen atom of the amino alcohol ligand coordinates to zinc (**1**, Scheme 2).[1f,n,5a,6b−d] Complex **1** acts as a bifunctional catalyst, where an aldehyde substrate coordinates to the Lewis acidic zinc (the catalytic zinc), and the Lewis basic oxygen coordinates to a dialkylzinc reagent (**2**, Scheme 2).[1m,5,6c,7] The catalytic cycle proceeds via a stable preproduct complex (**3**, Scheme 2) with a four-membered Zn−O−Zn−O ring. However, this does not cause product inhibition, because the product can dissociate from the catalyst and form very stable tetramers and dimers (Scheme 2).[1m,5a]

Many ligands that promote the title reaction enantioselectively show a nonlinear relationship between ligand purity (or catalyst purity) and product purity − so-called chiral or asymmetric amplification.[1l,m,2b,3q,6b−d,8] This nonlinearity is believed to arise from a reversible equilibrium between the two enantiomers that act as active catalysts (**1**) and their catalytically inactive dimers.[1m,2b,6b−d,9] With a nonracemic ligand (catalyst), the heterodimer of the chiral complex **1** is so stable that it quite effectively suppresses one of the two enantiomorphic pathways − the one requiring the minor enantiomer ligand as catalyst, leading to very large asymmetric amplification. However, recently the inverse effect, asymmetric depletion, has also been observed.[10]

The aldehyde can coordinate to the catalytic zinc with either of its two lone pairs − cis or trans to R′ − and from either face of the almost planar zinc atom in complex **1**, leading to two diastereomeric pairs of complex **2**, as shown in Figure 1.

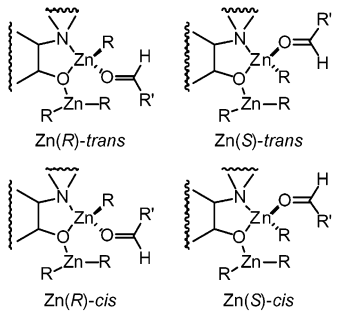

Figure 1. Different coordination modes of the aldehyde to the catalyst. We always use the following priorities for assigning the stereochemistry of the catalytic zinc: alkoxide-O > aldehyde-O > N > R.

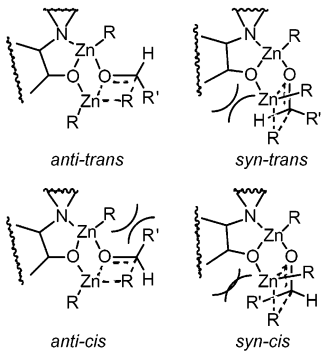

Figure 2. Tricyclic transition states for the Zn(*R*) face. The terms syn and anti define the relationship between the transferring alkyl and the bidentate ligand, whereas cis and trans define which aldehyde lone pair coordinates to the catalytic zinc.[7]

Several types of transition states (TSs) have been proposed in the literature,[1f,j,m,n,2a,b] but the consensus seems to have settled on a mechanism proposed by Yamakawa and Noyori. In their 1995 paper, they present a theoretical investigation of a small model system consisting of dimethylzinc, formaldehyde, and 2-aminoethanol.[5a] They characterized two tricyclic transition states − syn and anti orientation of the terminal rings − and one bicyclic TS. MP2[5a] and B3LYP[11] calculations show that the tricyclic anti configuration is the most favored, being 12−13 kJ mol^{-1} more stable than the tricyclic syn configuration, and 29 kJ mol^{-1} more stable than the bicyclic TS. When the mechanism proceeds via the tricyclic transition states, alkyl migration occurs with retention of configuration on the migrating alkyl carbon. Conversely, the high-energy bicyclic pathway would lead to migration with inversion of configuration.[5a]

The chiral ligand will favor one face of the catalytic zinc over the other. For the favored zinc face, there are four potential tricyclic transition states (anti-trans, anti-cis, syn-trans, and syn-cis), as shown in Figure 2 for the Zn(*R*) face. In general, the most favorable of these configurations is the anti-trans (vide infra). The minor enantiomer can arise via the syn-trans or anti-cis pathways, whereas syn-cis (leading to the same product as anti-trans) is highly disfavored due to steric crowding. Generally, the syn pathways are disfavored due to steric repulsion between the ligand and both the aldehyde and the migrating alkyl. For the disfavored face of the catalytic zinc, only the anti-trans configuration, which leads to minor enantiomer formation, will normally be important. We will call this configuration inv-anti-trans, due to the inversion of configuration on the catalytic zinc.[12]

(4) (a) Dosa, P. I.; Ruble, J. C.; Fu, G. C. *J. Org. Chem.* **1997**, *62*, 444−445. (b) Huang, W.-S.; Pu, L. *J. Org. Chem.* **1999**, *64*, 4222−4223. (c) Bolm, C.; Muñiz, K. *Chem. Commun.* **1999**, 1295−1296. (d) Bolm, C.; Hildebrand, J. P.; Muñiz, K.; Hermanns, N. *Angew. Chem., Int. Ed.* **2001**, *40*, 3284−3308. (e) Bolm, C.; Hermanns, N.; Kesselgruber, M.; Hildebrand, J. P. *J. Organomet. Chem.* **2001**, *624*, 157−161. (f) Zhao, G.; Li, X.-G.; Wang, X.-R. *Tetrahedron: Asymmetry* **2001**, *12*, 399−403. (g) Ko, D.-H.; Kim, K. H.; Ha, D.-C. *Org. Lett.* **2002**, *4*, 3759−3762. (h) Bolm, C.; Rudolph, J. *J. Am. Chem. Soc.* **2002**, *124*, 14850−14851.

(5) (a) Yamakawa, M.; Noyori, R. *J. Am. Chem. Soc.* **1995**, *117*, 6327−6335. (b) Yamakawa, M.; Noyori, R. *Organometallics* **1999**, *18*, 128−133.

(6) (a) Kitamura, M.; Suga, S.; Niwa, M.; Noyori, R.; Zhai, Z.-X.; Suga, H. *J. Phys. Chem.* **1994**, *98*, 12776−12781. (b) Kitamura, M.; Suga, S.; Niwa, M.; Noyori, R. *J. Am. Chem. Soc.* **1995**, *117*, 4832−4842. (c) Kitamura, M.; Suga, S.; Oka, H.; Noyori, R. *J. Am. Chem. Soc.* **1998**, *120*, 9800−9809. (d) Kitamura, M.; Oka, H.; Noyori, R. *Tetrahedron* **1999**, *55*, 3605−3614.

(7) We use the terms "catalytic zinc" to designate the zinc atom permanently coordinated to the bidentate ligand, "substrate" for the reacting aldehyde, and "reagent" for the dialkyl zink species that is coordinated to the oxygen of the catalyst for part of the catalytic cycle. The α-position designates the carbon directly connected to the alkoxide oxygen, whereas the β-position is the backbone carbon atom bound directly to the nitrogen.

(8) Soai, K.; Shibata, T. Asymmetric Amplification and Autocatalysis. In *Catalytic Asymmetric Synthesis*, 2nd ed.; Ojima, I., Ed.; Wiley-VCH: New York, 2000; pp 699−725.

(9) The catalyst dimers need not be inactive for other types of ligands: Blackmond, D. G.; McMillan, C. R.; Ramdeehul, S.; Schorm, A.; Brown, J. M. *J. Am. Chem. Soc.* **2001**, *123*, 10103−10104.

(10) Steigelmann, M.; Nisar, Y.; Rominger, F.; Goldfuss, B. *Chem.-Eur. J.* **2002**, *8*, 5211−5218.

(11) Rasmussen, T.; Norrby, P.-O. *J. Am. Chem. Soc.* **2001**, *123*, 2464−2465.

For many ligands, experiments have identified key structural elements with respect to enantioselectivity, and a structure−selectivity relationship has hence been established. However, only in a limited number of cases is the source of the structure−selectivity relationship understood in detail. Such detailed insight is most readily provided by theoretical investigations, and a number of computational investigations into the origin of the enantioselectivity have been presented in the past decade.[5b,13] Here we present a detailed theoretical investigation of the selectivity determining interactions for a series of β-amino alcohol ligands, using a Q2MM force field.[14]

Methods

The many potentially important TS configurations and each configuration's numerous potentially significant conformations make a thorough theoretical investigation using ab initio and DFT methods very time-consuming and computationally demanding, for all but the simplest model systems. Conversely, the investigation of even a very large number of conformations is readily achievable with molecular mechanics (MM) methods, provided that a good force field exists for the system under investigation. However, MM methods are in general limited to the description of the stable conformers of a given molecular system and cannot be used to study bond forming and bond breaking transition states. A few methods are available for overcoming this limitation.[15] Here, we have chosen the established method of treating the TS as a minimum in the force field.[16] Such a TS force field has the advantage that all optimization and conformational search algorithms available for the investigation of minima can be used unmodified for the investigation of transition states. Obtaining a reliable TS force field often requires considerable parameter development, but the final tool allows *and* facilitates a rapid and fairly accurate screening of possible transition states for a given system.[16] We have recently applied TS force fields derived entirely from high level QM results (the Q2MM method[14]) to the HWE[17] and AD[18] reactions, demonstrating that this type of force field can be accurate to within a few kJ mol^{-1} when applied to stereoselectivity predictions.

In the present work, we have developed a TS force field for the tricyclic transition states described above, by augmenting the parameters of the MM3 force field,[19] as implemented in the MacroModel program[20] (MM3*). The additional parameters were developed in keeping with the Q2MM procedure, which we have detailed in a number of previous publications.[14,17,18,21] In this procedure, we achieve the transformation from saddle point to minimum by using modified Hessian elements as reference data in the parametrization procedure.[14,21] The original Hessian elements, and all other reference data, are obtained from DFT calculations on generic achiral model systems. Substituting the negative eigenvalue of the original TS Hessian with a large positive value results in a Hessian that corresponds to a minimum with steep sides in the direction of the former reaction coordinate. In other words, the curvature of the energy in the direction of the reaction coordinate is inverted at the position of the TS, and the TS is hence treated as a minimum.[21] The force field will react to distortions along the reaction coordinate with large energy increases, whereas distortions perpendicular to the reaction coordinate will be treated in a way that corresponds to results from the DFT calculations. Atoms involved in the formation and breaking of bonds will have limited flexibility in the TS force field, due to the high potential along the reaction coordinate. Such restrained flexibility of atoms involved in the reaction mode is necessary, because the treatment of a TS (a first-order saddle point) as a minimum results in an incorrect response to steric strain along the reaction coordinate.[14]

Parametrization Details. A total of 52 316 data points constitute the reference data set. An overview of the data set is available as Supporting Information. The reference data are distributed over bond lengths, bond angles, torsional angles, inverse interatomic distances, energy differences, Hessian elements, and ChelpG[22] charges, for 17 structures. All calculations were performed at the B3LYP[23] level using the 6-311+G basis set for zinc and the 6-31G* basis set for other atoms. The Gaussian 94 program[24] was used for all of the QM calculations that went into creating the reference data set. The generic model system is composed of 2-aminoethanol, dimethylzinc, and formaldehyde, but we have also included substituted structures to allow for the determination of parameters needed for larger systems. Parameters required for phenyl substituents have been obtained from QM calculations on the corresponding vinyl analogues. As ligands, we have included 2-(dimethylamino)-ethanol, 2-diallylamino-ethanol, and 2-(1-methyl-1-aziridinyl)-ethanol. Some structures derived from diethylzinc are also included. Finally, we have included all important orientations of acetaldehyde, as well as both propanal and propenal (acrolein). The latter is the simplest model that allows for the determination of parameters for conjugated aldehydes.

The parameters were optimized by minimizing a penalty function, defined as the sum of weighted squared deviations between MM calculated data and the reference data.[25] The weights are used primarily to scale the various types of reference data to a common order of magnitude, but are also used to make the penalty function unitless. In the present work, we used the reciprocal of an "acceptable" error in a specific data type as a guideline for determining the weight factor for these data type.[26] For example, the desired accuracy for reproduction of bond length reference data was set to ± 0.01 Å, giving a weight factor of 100 $Å^{-1}$ for bond length data. However, acceptable error is not the only consideration; it is also important to consider the number of the specific type of reference data points. Thus, the abundant Hessian elements were given relatively low weights to avoid that they become too dominant. Furthermore, Hessian elements in a 1,4-relationship were given higher weight than other Hessian elements, because these reference data are particularly important for the determination of torsional parameters.[27] All of the weight factors are shown in Table 1. Some parameters were tethered to a "reasonable" value with a harmonic

(12) Note that inv implies that the substrate and reagent coordinate to the face of the catalyst with the highest steric bulk.
(13) (a) Vidal-Ferran, A.; Moyano, A.; Pericàs, M. A.; Riera, A. *Tetrahedron Lett.* **1997**, *38*, 8773−8776. (b) Goldfuss, B.; Houk, K. N. *J. Org. Chem.* **1998**, *63*, 8998−9006. (c) Goldfuss, B.; Steigelmann, M.; Khan, S. I.; Houk, K. N. *J. Org. Chem.* **2000**, *65*, 77−82. (d) Goldfuss, B.; Steigelmann, M.; Rominger, F. *Eur. J. Org. Chem.* **2000**, 1785−1792. (e) Vázquez, J.; Pericàs, M. A.; Maseras, F.; Lledós, A. *J. Org. Chem.* **2000**, *65*, 7303−7309. (f) Panda, M.; Phuan, P.-W.; Kozlowski, M. C. *J. Org. Chem.* **2003**, *68*, 564−571.
(14) Norrby, P.-O. *J. Mol. Struct. (THEOCHEM)* **2000**, *506*, 9−16.
(15) Jensen, F.; Norrby, P.-O. *Theor. Chem. Acc.* **2003**, *109*, 1−7.
(16) Eksterowicz, J. E.; Houk, K. N. *Chem. Rev.* **1993**, *93*, 2439−2461.
(17) Norrby, P.-O.; Brandt, P.; Rein, T. *J. Org. Chem.* **1999**, *64*, 5845−5852.
(18) (a) Norrby, P.-O.; Rasmussen, T.; Haller, J.; Strassner, T.; Houk, K. N. *J. Am. Chem. Soc.* **1999**, *121*, 10186−10192. (b) Fristrup, P.; Tanner, D.; Norrby, P.-O. *Chirality* **2003**, *15*, 360−368.
(19) Allinger, N. L.; Yuh, Y. H.; Lii, J.-H. *J. Am. Chem. Soc.* **1989**, *111*, 8551−8566.
(20) Mohamadi, F.; Richards, N. G. J.; Guida, W. C.; Liskamp, R.; Lipton, M.; Caulfield, C.; Chang, G.; Hendrickson, T.; Still, W. C. *J. Comput. Chem.* **1990**, *11*, 440−467.
(21) Norrby, P.-O. In *Molecular Mechanics as a Predictive Tool in Asymmetric Catalysis*; Truhlar, D. G., Morokuma, K., Eds.; American Chemical Society: Washington, DC, 1999; pp 163−172.
(22) Breneman, C. M.; Wiberg, K. B. *J. Comput. Chem.* **1990**, *11*, 361−373.
(23) (a) Lee, C.; Yang, W.; Parr, R. G. *Phys. Rev. B* **1988**, *37*, 785−789. (b) Becke, A. D. *J. Chem. Phys.* **1993**, *98*, 5648−5652.
(24) Frisch, M. J.; Trucks, G. W.; Schlegel, H. B.; Gill, P. M. W.; Johnson, B. G.; Robb, M. A.; Cheeseman, J. R.; Keith, T.; Petersson, G. A.; Montgomery, J. A.; Raghavachari, K.; Al-Laham, M. A.; Zakrzewski, V. G.; Ortiz, J. V.; Foresman, J. B.; Cioslowski, J.; Stefanov, B. B.; Nanayakkara, A.; Challacombe, M.; Peng, C. Y.; Ayala, P. Y.; Chen, W.; Wong, M. W.; Andres, J. L.; Replogle, E. S.; Gomperts, R.; Martin, R. L.; Fox, D. J.; Binkley, J. S.; Defrees, D. J.; Baker, J.; Stewart, J. P.; Head-Gordon, M.; Gonzalez, C.; Pople, J. A. *Gaussian 94*, revision E.2; Gaussian, Inc.: Pittsburgh, PA, 1995.
(25) Norrby, P.-O.; Liljefors, T. *J. Comput. Chem.* **1998**, *19*, 1146−1166.
(26) (a) Norrby, P.-O.; Brandt, P. *Coord. Chem. Rev.* **2001**, *212*, 79−109. (b) Norrby, P.-O. Recipe for an Organometallic Force Field. In *Computational Organometallic Chemistry*; Cundari, T., Ed.; Marcel Dekker: New York, 2001; pp 7−37.
(27) Maple, J. R.; Hwang, M.-J.; Stockfisch, T. P.; Dinur, U.; Waldman, M.; Ewig, C. S.; Hagler, A. T. *J. Comput. Chem.* **1994**, *15*, 162−182.

Table 1. Weight and Tethering Factors

ref data type	weight factor	unit
bond length	100	$Å^{-1}$
bond angle	2	$(deg)^{-1}$
torsional angle	1	$(deg)^{-1}$
inverse distance	20	Å
torsional drive	1 or 2	mol kJ^{-1}
config. energy diff.	5	mol kJ^{-1}
Hessian element	0.005	mol amu $Å^2$ kJ^{-1}
1,4-Hessian element	0.05	mol amu $Å^2$ kJ^{-1}
charge	50	au^{-1}

parameter type	tethering factor	unit
θ_0	2	$(deg)^{-1}$
k_b	5	rad^2 $mdyn^{-1}$
v_n	1	mol $kcal^{-1}$
vdW radius	3	$Å^{-1}$
vdW ϵ	15	mol $kcal^{-1}$

potential, to aid the optimization. Again, we used the reciprocal of an acceptable deviation from the chosen value as a guideline for determining the tethering factors.[26] The tethering factors are also shown in Table 1. The θ_0 angle parameters were tethered toward the average of the corresponding QM bond angles, and bend force constants were tethered toward a value 0.5 mdyn rad^{-2}. All torsional parameters were tethered toward a value of 0.0 kcal mol^{-1}. In addition, the vdW radius and hardness of Zn were tethered toward 2.29 Å and 0.276 kcal mol^{-1}, respectively.[28] In the final stages of the parameter optimization, all tetherings were relaxed for a few iterations. Initially, 197 additional MM3* parameters were optimized; however, 19 of these parameters were zeroed after optimization, due to very small final values. The refined MM3* parameters are available as Supporting Information.

Computational Details. All selectivities were calculated using Boltzmann averages of MM potential energies of structures obtained from an unbiased conformational search for all low-energy conformations. The MM calculations were performed with MacroModel v. 6.0[20] on Silicon Graphics workstations running IRIX 6, using the augmented MM3* force field described above. To create the conformational ensemble, input structures for each of the tricyclic TS-configurations (i.e., anti-trans, anti-cis, syn-trans, and syn-cis) were generated. Not to bias the conformational search, each input structure was separately subjected to a combination of the initial pseudo-systematic Monte Carlo search[29] and the subsequent Low Mode search.[30] The former method searches all parts of the conformational space, initially using a coarse resolution for the rotation of free torsions. Whenever possible, enough steps were performed to allow all combinations of torsional angles to be tested while using the coarse resolution. The default step size is 120°, which requires at least 3^N steps to test all combinations, where N is the number of free torsions. In the cases where $N > 8$, only the 8 most important torsions were included, and 10 000 steps were performed. The resulting conformers were then subjected to a normal Monte Carlo search, testing only variations in the remaining torsions. The Low Mode method searches the local region around the input structures, and hence the two methods complement each other excellently. The number of steps taken in the Low Mode search was set to 3 times the number of structures in the input file, that is, 3 times the number of conformers generated by the Monte Carlo search. During these conformational searches, all conformers within 100 kJ mol^{-1} of the global minimum were stored. After the Low Mode search, the ensembles of TS-configurations leading to *S*-products were collected in one file, as were ensembles of TS-configurations leading to *R*-products. These files were then reminimized to ensure well-converged structures for all conformers. This time, only conformers within 30 kJ mol^{-1} of the global minimum were kept.[31] Finally, the relative rate between the two pathways (*R* and *S*) was obtained from the Boltzmann distribution of each ensemble, using the reaction temperature reported for the specific ligand. The remaining entropy contributions and solvation contributions were ignored.

To aid the analysis of the MM structures, we compared them with earlier B3LYP/LACVP* calculations[11,23,32] for a generic system composed of dimethylamino-ethanol, dimethylzinc, and acetaldehyde. These calculations were performed in Jaguar v4.0 or v4.1.[33]

Chart 1. Ligands Studied with the Force Field

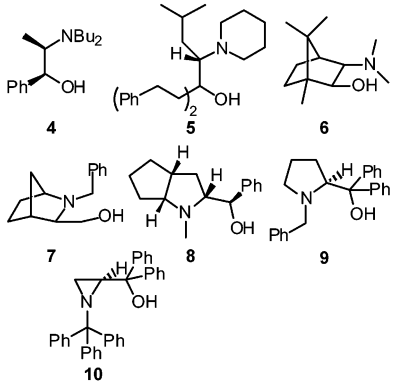

Chart 2. Substrates Studied with the Force Field

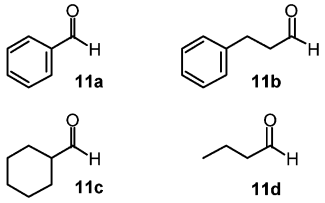

Results and Discussion

The developed force field was used to study the set of ligands shown in Chart 1. Ligands **4** (DBNE)[1g] and **6** (DAIB)[1e] were among the first ligands shown to have high selectivity for the title reaction. Ligands **5**, **7**, **8**, and **9** have been studied by Kawanami et al.,[3m] Guijarro et al.,[3d] Martens and co-workers,[3g,34] and Yang et al.,[3f] respectively. Ligands very similar to **9** have been studied already in the late 1980s by Soai et al.[3h,i]

Generally, most ligands show higher selectivity with aromatic aldehydes than with aliphatic aldehydes.[2] Ligand **10** is one of the few ligands known to be highly selective with both aromatic and aliphatic aldehydes.[3i] However, the ligand showed only moderate selectivity (80% ee) with the simple linear aliphatic aldehyde, heptanal. In the present work, both aromatic and aliphatic substrates were studied (Chart 2). The reagent is in all cases diethylzinc.

The enantioselectivities obtained with the force field model are presented in Table 2, along with the catalytic zinc face favored for aldehyde coordination (Figure 1)[7] and the energy differences between the favored pathway and the possible

(28) Allinger, N. L.; Zhou, X.; Bergsma, J. *J. Mol. Struct. (THEOCHEM)* **1994**, *312*, 69−83.
(29) Goodman, J. M.; Still, W. C. *J. Comput. Chem.* **1991**, *12*, 1110−1117.
(30) Kolossvary, I.; Guida, W. C. *J. Am. Chem. Soc.* **1996**, *118*, 5011−5019.
(31) The Low Mode method can invert chiral atoms, and the automatic chirality check implemented in MacroModel v. 6.0 to avoid this inversion cannot handle the almost planar atom, which is responsible for the forming chirality. Hence, filtering is usually required after the Low Mode search, to ensure that only the desired forming chirality is present.
(32) The LACVP* basis set uses 6-31G* for light elements and the Hay−Wadt ECP for Zn: Hay, P. J.; Wadt, W. R. *J. Chem. Phys.* **1985**, *82*, 270−283.
(33) http://www.schrodinger.com.
(34) (a) Wilken, J.; Gröger, H.; Kossenjans, M.; Martens, J. *Tetrahedron: Asymmetry* **1997**, *8*, 2761−2771. (b) Wilken, J.; Kossenjans, M.; Gröger, H.; Martens, J. *Tetrahedron: Asymmetry* **1997**, *8*, 2007−2015.

Table 2. Calculated and Experimental Enantioselectivities

entry	ligand	aldehyde (R′–CHO)	favored Zn face[a]	cost of change (kJ mol^{-1})[b] inv	syn	cis	ee$_{cal}$[c]	ee$_{exp}$	ref
1	**4**	**11a** (Ph)	Zn(*R*)	>30	15	21	99.8	90 (*S*)	1g
2	**4**	**11c** (Cy)	Zn(*R*)	>30	21	14	99.7	78 (*S*)	1g
3	**5**	**11a** (Ph)	Zn(*S*)	10	14	15	96.9	97 (*R*)	3m
4	**6**	**11a** (Ph)	Zn(*R*)	>30	13	19	99.3	98 (*S*)	1e
5	**6**	**11b** (PhEt)	Zn(*R*)	>30	13	4	84.1	90 (*S*)	1e
6	**6**	**11d** (Pr)	Zn(*R*)	>30	16	4	74.4	61 (*S*)	1e
7	**7**	**11a** (Ph)	Zn(*R*)	16	9	21	92.7	75 (*S*)	3d
8	**8**	**11a** (Ph)	Zn(*S*)	15	24	22	98.8	68 (*R*)	3g
9	**9**	**11a** (Ph)	Zn(*R*)	2	>30	18	45.9	81.8 (*S*)	3f
10	**10**	**11a** (Ph)	Zn(*R*)	20	>30	14	99.5	99 (*S*)	3i

[a] All favored pathways have anti-trans configuration. Consult Figures 1 and 2 for definitions of stereochemical labels. [b] Difference in energy between the lowest-energy conformer with anti-trans configuration and the lowest-energy conformer with inv-anti-trans, syn-trans, or anti-cis configuration. [c] The qualitative selectivity (*R*/*S*) is correct in all cases.

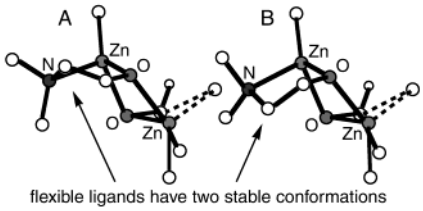

Figure 3. Stable chelate ring conformations for the generic system. Note that an inversion of the configuration on the catalytic zinc will turn conformer A into conformer B and vice versa.

pathways to the minor enantiomer. The major enantiomer is in each case generated by an anti-trans pathway. Ligands **4** and **6** block one face of the catalytic zinc very effectively, whereas ligands **9** and **10** effectively block the syn-trans pathway (columns 5 and 6, Table 2). The blocking of the anti-cis pathway shows a strong substrate dependency, being much less pronounced with aldehydes **11b** and **11d**, which have limited bulk close to the carbonyl bond (column 7, Table 2). Conversely, this pathway is disfavored by more than 10 kJ mol^{-1} when the substrate is benzaldehyde (**11a**) or has substantial bulk close to the carbonyl bond (**11c**). For the substrate benzaldehyde, the anti-cis pathway is the favored route to minor enantiomer formation only in the case of ligand **10**, which is the most selective ligand included in the study. The ligands that block one face of the catalytic zinc effectively (**4** and **6**) have chirality that favor the same catalyst face on both of the β-amino alcohol backbone carbons, which is not the case for any of the other ligands (Chart 1). Ligands **9** and **10**, which block the syn-trans pathway effectively, both have two phenyl substituents on the α-carbon and a short bridge linking the β-carbon and the nitrogen.[7] The latter structural feature, which is also present in ligand **8** that likewise shows a high barrier for the syn-trans pathway, is the determining factor (vide infra).

Considering first the B3LYP results for the generic system consisting of β-dimethylamino ethanol, acetaldehyde, and dimethylzinc, we find two stable conformations of the five-membered chelate ring. One conformer has eclipsed conformations along the N−Zn bond and the C$_\alpha$−O bond (conformer A, Figure 3), whereas the other conformer has staggered conformations for all chelate ring bonds (conformer B, Figure 3). The coordination of both substrate and reagent is slightly disfavored in conformer A as compared with that in conformer B. In conformer A, there is higher steric interaction between an

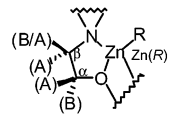

Figure 4. Favored chelate ring conformer for the various α- and β-carbon monosubstitutions.

N-substituent and the substrate − for the anti configuration, the interaction is only with the oxygen part of the carbonyl bond, whereas for the syn configuration, the interaction is with the entire carbonyl part of the substrate. Moreover, the spectator alkyl on the catalytic zinc is slightly closer to an N-substituent in conformer A than in conformer B. However, for the syn configuration, the β-carbon comes close to the reaction site in conformer B. The B3LYP calculations show that conformer B is ca. 4 kJ mol^{-1} more stable than conformer A for both the anti-trans and the anti-cis configurations, whereas conformer B is favored by only ca. 2 kJ mol^{-1} for the syn-trans and the syn-cis configurations.

For both conformers A and B, an α-carbon substituent will produce steric interaction with a reagent coordinating to the face of the catalyst with the α-carbon substituent. However, in conformer B, the steric interaction will primarily involve the zinc atom of the reagent, whereas in conformer A, the steric interaction will involve both the zinc atom and an alkyl moiety of the reagent due to the more axial position of the substituent in this conformer. From the generic system, it is also clear that a β-carbon substituent on the face of the catalyst where the substrate and reagent coordinates will favor conformer A, because in conformer B the substituent will interact strongly with both the substrate and the reagent due to the more axial position of the substituent in conformer B. Furthermore, an α-carbon substituent on the face of the catalyst opposite to the coordinating reagent will favor conformer A due to steric interaction with an N-substituent in conformer B, where both the N-substituent and the α-carbon substituent will be in axial positions. Conversely, it is not apparent which conformer would be favored with a β-carbon substituent on the face opposite to the coordinating reagent and substrate, because this substituent will have steric interaction with an N-substituent in both conformers. However, it is clear that an α- or a β-carbon substituent in an axial position is disfavored in general. The rationalizations presented above are summarized in Figure 4. Ligands **4** and **5** have no locked torsions in the β-amino alcohol part and can in principle adapt both stable chelate ring conformations described above, whereas the remaining ligands included in the study all have one locked torsion in the β-amino alcohol part.

We will now discuss in further detail the specific pathways for minor enantiomer product formation (i.e., inv-anti-trans, syn-trans, and anti-cis) and the individual characteristics of the various ligands. For each path, we discuss in turn each ligand for which the path would be the most important source of the minor enantiomer, in the order in which they appear in Table 2.

Inv-anti-trans. Ligand **5** does not differentiate effectively between the two faces of the catalytic zinc and hence gives way for anti-trans configurations utilizing both zinc faces (Figure 5). The minor enantiomer product is predicted to be formed mainly through the inv-anti-trans pathway also for ligands **8** and **9**. Although these ligands leave the catalyst partially open

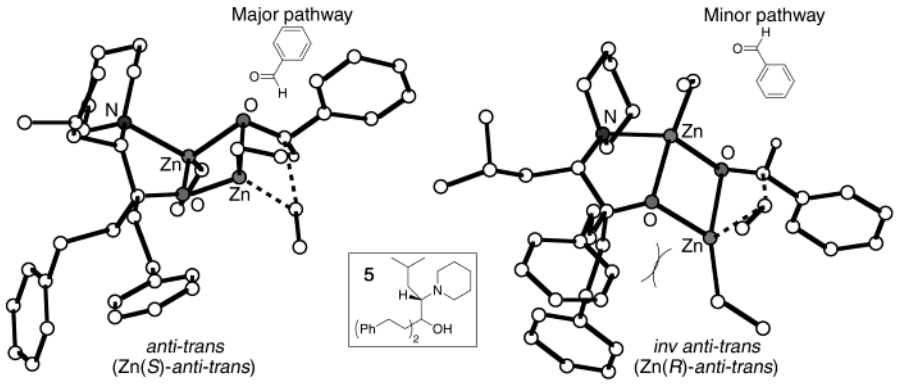

Figure 5. Stereodifferentiation by substrate coordination to either face of the catalyst.

to substrate and reagent coordination at both zinc faces, the selectivity can be quite high (e.g., 97% ee, ligand **5**, entry 3, Table 2). In the case of ligand **5**, the CH_2CH_2Ph α-carbon substituents minimize steric interaction with the zinc and spectator part of the reagent in chelate ring conformer B (see above). Hence, the pathway to the major enantiomer product (i.e., Zn(*S*)-anti-trans) has chelate ring conformation B. For the pathway to the minor enantiomer product (i.e., Zn(*R*)-anti-trans), the chirality of the *β*-carbon controls which of the two chelate ring conformers is the favored, because in conformer B the *β*-carbon substituent has strong steric interaction with both the coordinating substrate and the reagent. Hence, the preferred chelate ring conformer for the minor pathway with ligand **5** is conformer A, which has one of the α-carbon substituents in an unfavorable position relative to the reagent and an eclipsed conformation along the N−Zn bond. The latter structural characteristic seems to be less significant, and the destabilizing effects for the minor pathway thus primarily arise from steric interaction between a CH_2CH_2Ph moiety of the ligand and the zinc plus spectator alkyl part of the reagent (Figure 5).

Ligand **8** locks the chelate ring conformation in what corresponds to conformer A for substrate and reagent coordination to the Zn(*S*) face of the catalyst (major pathway, i.e., Zn-(*S*)-anti-trans) and to conformer B for coordination to the inverse face (minor pathway, i.e., Zn(*R*)-anti-trans). There is no α-carbon substituent on the Zn(*S*) face of the catalyst, so reagent coordination to this face is facile. However, substrate coordination is more facilitated at the Zn(*R*) face of the catalyst, due to the chelate ring conformation (see above). Conversely, coordination of the reagent is hindered at the Zn(*R*) face due to the α-carbon phenyl substituent, so even though substrate coordination is not optimal at the Zn(*S*) face, it is the preferred catalyst face. Thus, the most significant destabilizing effect is the steric interaction between the phenyl moiety of the ligand and the zinc atom as well as, to some extent, the spectator alkyl of the reagent. The model predicts the ligand to be highly selective, which is in discrepancy with the experimental selectivity (entry 8, Table 2). However, the model also indicates that the substrate coordination is not optimal in the major pathway and in that way implies problems with the ligand.

Ligand **9** is unique in that it can chelate to zinc also after inversion of the nitrogen (a facile process in the free ligand). Hence, although the bridge linking the *β*-carbon and the nitrogen locks the chelate ring conformation, it can adapt the preferred conformation (conformer B) for substrate and reagent coordination to both zinc faces. Reagent coordination is nearly equally hindered at both faces due to the two α-carbon phenyl substituents. One epimer of the ligand has a phenyl group interacting with the pyrrolidine ring (minor pathway, i.e., Zn-(*S*)-anti-trans), whereas the other epimer has a phenyl group interacting with the *N*-benzyl moiety (major pathway, i.e., Zn-(*R*)-anti-trans). In addition, the differentiation between the major and the minor pathway is also governed by the difference in steric interaction, involving the substrate and the spectator alkyl on the catalytic zinc, between the two pathways. In the minor pathway, the substrate interacts with the *N*-benzyl substituent, whereas the substrate interacts with the pyrrolidine part of the ligand in the major pathway. However, in the major pathway, there is some steric interaction between the *N*-benzyl substituent and the spectator alkyl on the catalytic zinc and between the pyrrolidine ring and the reagent. That is, the model clearly indicates that the ligand should not be highly selective, giving only ca. 2 kJ mol^{-1} preference for one pathway over the other. Indeed, the ligand is not highly selective, but it is slightly more selective than that predicted by the model (entry 9, Table 2).

Experiments have shown that a substitution of *N*-benzyl with *N*-methyl for this ligand increases the enantiomeric excess from 82% to 96% for the addition of diethylzinc to benzaldehyde.[35] This experimental observation is in good accordance with our force field model, because the *N*-methyl substituent will reduce steric interaction significantly more for the major pathway than for the minor pathway. Especially the steric repulsion between the N-substituent and the spectator alkyl on the catalytic zinc will be reduced for the major pathway.

Syn-trans. Returning to the generic system described above, we now analyze the syn configuration. As compared with the anti configuration, the steric interaction between the coordinating substrate and the N-substituent has increased considerably. In the syn configuration, the other alkyl of the reagent as compared with that in the anti configuration is utilized for alkyl migration, which significantly alters the substrate orientation relative to the ligand. This altered substrate orientation brings the entire carbonyl part of the substrate in close proximity to the ligand. In addition, the interaction between the spectator alkyl on the catalytic zinc and the other N-substituent has also increased slightly. As mentioned, the alkyl that is a spectator in the anti configuration is the migrating alkyl in the syn configuration, which slightly increases the steric interaction between this alkyl and the ligand. As for the anti configuration, chelate ring conformer B is slightly favored over conformer A (see above).

(35) Liu, G.; Ellman, J. A. *J. Org. Chem.* **1995**, *60*, 7712−7713.

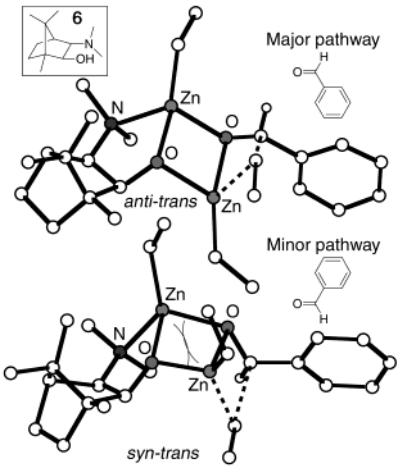

Figure 6. Anti−syn stereodifferentiation with substrate coordinating to the same face of the catalyst.

Ligand **4** blocks the Zn(*S*) face of the catalyst very effectively due to substituents on both the α- and the *β*-carbon favoring the Zn(*R*) face. Thus, minor enantiomer products must be formed via either the syn-trans or the anti-cis pathway, utilizing the Zn(*R*) face of the catalyst. With the benzaldehyde substrate (**11a**), minor enantiomer is generated via the syn-trans pathway (entry 1, Table 2). The α-carbon substituent, phenyl, favors conformer A, because in conformer B it has a strong steric interaction with an N-substituent. Hence, the chelate ring is in effect locked in conformation A. As described above for the generic system, the differentiation between the major and the minor pathway is primarily governed by the increased steric interaction between the ligand and the substrate in the syn-trans configuration (see, e.g., Figure 6).

Ligand **6** is quite similar to ligand **4** − it blocks the Zn(*S*) face of the catalyst very effectively, having chirality favoring the Zn(*R*) face on both the α- and the *β*-carbon. Furthermore, ligand **6** locks the chelate ring in a conformation most comparable with that of conformer A. However, the N−C_β−C_α−O torsional angle is locked at ca. 25°, whereas it is around 46° in the generic system. Ligand **6** differs from ligand **4** by having the rigid frame of isoborneol, which prevents any relaxation of steric interactions with substrate and reagent. This rigid frame is probably the reason for the experimentally observed higher selectivity of ligand **6** as compared with that of ligand **4** (Table 2). Our static TS model is apparently not able to differentiate correctly between ligands **4** and **6**. This inaccuracy could rely on the partial neglect of entropy contributions in the current model. Because ligand **4** has a greater number of flexible torsions than ligand **6**, it is likely that there is a more significant entropy difference between the major and the minor pathway for ligand **4**. We have also speculated that the recently characterized six-membered transition states were important for formation of minor enantiomer products with ligand **4** and not with ligand **6**,[11] but an ongoing investigation with DFT and QM/MM indicates that six-membered transition states are unimportant for both ligands.[36] As with ligand **4**, minor enantiomer is generated via the syn-trans pathway for the substrate benzaldehyde (**11a**) with ligand **6** (Figure 6).

(36) Rasmussen, T.; Dölker, N.; Maseras, F.; Norrby, P.-O., manuscript in preparation.

The force field results for ligand **6** (DAIB) compare well with results obtained by Yamakawa and Noyori for Hartree−Fock (HF) and B3LYP calculations on a system consisting of DAIB, dimethylzinc, and benzaldehyde.[5b] The HF results give the same ordering of TS stabilities as the force field (i.e., anti-trans > syn-trans > anti-cis), however, with a slightly smaller favoring of the anti-trans pathway than was found with the force field, whereas the B3LYP results show a disfavoring by ca. 15 kJ mol^{-1} of both the syn-trans and the anti-cis pathway as compared with the anti-trans pathway. For HF, the syn-trans and the anti-cis pathways are disfavored as compared with the anti-trans pathway by 11 and 15 kJ mol^{-1}, respectively. The force field model gives a disfavoring, as compared with the anti-trans pathway, of 13 kJ mol^{-1} for the syn-trans pathway and 19 kJ mol^{-1} for the anti-cis pathway.

Ligand **7** locks the chelate ring in a conformation that resembles conformer A more than conformer B. In fact, the N−C_β−C_α−O torsional angle is almost the same as that for conformer A of the generic system in both the major and the minor pathway. However, the position of the catalytic zinc relative to the plane spanned by N, C_α, and O is shifted significantly as compared with that of the generic system. In the generic system, the angle of the Zn, N, C_α plane relative to the N, C_α, O plane is ca. 10° counterclockwise, whereas it is ca. 10° clockwise with ligand **7**. The effect of the shifted zinc position relative to the ligand propagates to both the substrate and the reagent, which have markedly altered positions relative to the ligand, as compared with those of the generic system. The minor enantiomer is formed via the syn-trans pathway of the Zn(*R*) face, but the energy penalty for this pathway as compared with that of the anti-trans pathway is lower than that for ligands **4** and **6**. This reduction in energy penalty relies on the shifted position of the substrate relative to the ligand, which slightly reduces the steric interaction between the *N*-benzyl moiety and the benzaldehyde substrate.

Anti-cis. There is essentially no difference between anti-trans and anti-cis pathways with respect to how much direct steric interaction the substrate has with the ligand. Hence, destabilization of the anti-cis pathway is caused almost exclusively by steric interaction between the spectator alkyl on the catalytic zinc and the substrate substituent. For the generic system with acetaldehyde, B3LYP calculations show that this destabilization is less than 2 kJ mol^{-1} for both conformers A and B.

The aforementioned HF calculations (by Yamakawa and Noyori) indicate that there is almost perfect phenyl-carbonyl conjugation for benzaldehyde in the TS.[5b] Hence, it is quite apparent that it is much harder to block the anti-cis pathway for simple linear aliphatic aldehydes than for arylic aldehydes. The arylic aldehydes will have to abandon conjugation with the carbonyl bond to minimize steric interaction with the spectator alkyl on the catalytic zinc, whereas simple aliphatic aldehydes experience only moderate steric interaction with the catalytic zinc moiety (Figure 7). This description agrees well with the experimental observations that higher selectivity is obtained with arylic and substituted aliphatic aldehydes than with simple aliphatic aldehydes.

Although the destabilization of the anti-cis pathway primarily depends on the substrate, the force field model indicates that the interaction between the ligand N-substituent and the spectator alkyl on the catalytic zinc can play a role. Comparing, for

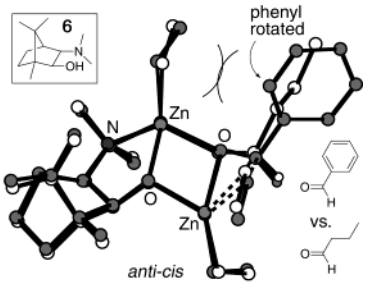

Figure 7. Destabilization of the anti-cis pathway for arylic aldehydes.

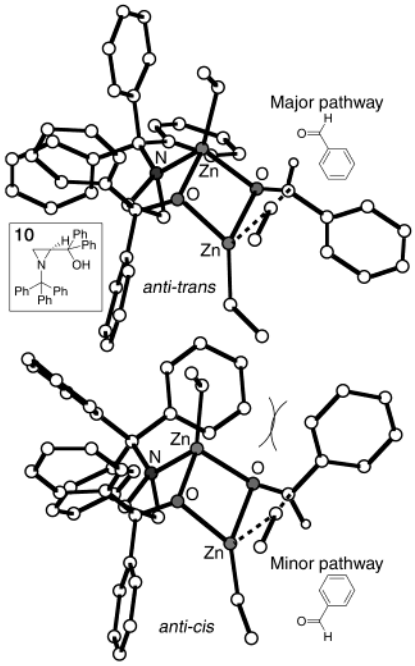

Figure 8. Trans−cis stereodifferentiation with substrate coordination to the same face of the catalyst.

example, entries 1 and 3 in Table 2 shows that the anti-cis pathway is more destabilized by ligand **4** than by ligand **5** for the same substrate, benzaldehyde. As mentioned earlier, ligand **4** locks the chelate ring in conformation A, which has a quite eclipsed conformation around the N−Zn bond, whereas ligand **5** locks the chelate ring in conformation B, which has a more staggered conformation around the N−Zn bond. Hence, the spectator alkyl on the catalytic zinc gets sandwiched more in one case than in the other. However, the force field model clearly suggests that a ligand, which enforces minor enantiomer formation via the anti-cis pathway, will give high selectivity with arylic aldehydes regardless of the magnitude of interaction between the ligand N-substituent and the catalytic zinc moiety. A good example of how to block both inv and syn pathways is ligand **10** (entry 10, Table 2).

Ligand **10** locks the chelate ring in a conformation where the N−C_β−C_α−O torsional angle resembles that of conformer B of the generic system. However, because of the strained aziridine structure, the conformation around the N−Zn bond is more comparable with what is found in conformer A of the generic system. The aziridine ring and the O−Zn−O−Zn ring are syn to each other for substrate coordination to the Zn(*R*) face, which places the unsubstituted vertex of the aziridine in an ideal position to block the syn-trans pathway (see Figure 8). Substrate coordination to the Zn(*S*) face is apparently hindered by the bulky *N*-trityl substituent, which then suppresses the inv-anti-trans pathway. Finally, the anti-cis pathway is destabilized by the steric interaction between the spectator alkyl on the catalytic zinc and the phenyl substituent of the substrate (Figure 9).

At this point, we would like to revisit the results presented in Table 2. Seven out of the 10 calculated selectivities are within 3 kJ mol^{-1} of the experimental result, which is high accuracy for a computational approach. The three remaining calculated selectivities (entries 1, 2, and 8 in Table 2) are off by 9−10 kJ mol^{-1}, which is still acceptable considering the simplicity of the theoretical approach and the variety of systems accommodated by the force field model. Furthermore, it is reassuring to note that the relative selectivity obtained for ligand 4 (entry 1 versus entry 2 in Table 2) is very accurate, albeit the absolute selectivities are less accurate. Because of the logarithmic relationship between the enantiomeric ratio and the energy difference between enantiomorphic transition states, the selectivity increase from 99.7 to 99.8 ee corresponds to the same energy difference as the increase from 78 to 90 ee. The favoring of the major enantiomer pathway is in both cases increased by ca. 2 kJ mol^{-1}. A higher-level computational investigation of the title reaction with ligand **4**, based on the important configurations and conformations located here, is currently in progress.[36]

Conclusions

We have established the structure−selectivity relationship for a series of β-amino alcohol promoters of the diethylzinc addition to aldehydes, by performing an extensive investigation of all possible Noyori type pathways with a Q2MM approach. For all studied systems, the major enantiomer product is formed via the anti-trans pathway, whereas the minor enantiomer product in general is formed via the inv-anti-trans or the syn-trans pathway for benzaldehyde and via the anti-cis pathway for aliphatic aldehydes. Only the most selective ligand (**10**) forces formation of the minor enantiomer product to occur via the anti-cis pathway for benzaldehyde.

The force field model indicates that a sufficient condition for obtaining fairly high selectivity with arylic aldehydes is that the ligand blocks one face of the catalyst reasonably well. That is, the ligand forces minor enantiomer product formation to occur via the syn-trans pathway. Ligand **7** is an apparent exception due to the altered coordination of the nitrogen to the catalytic zinc as compared with the situation in the generic system.

The model also indicates that blocking one face of the catalyst effectively requires chirality on both the α- and the β-carbon, which favors the same catalyst face. The α-carbon substituent is probably the most vital as this substituent is quite close to the reagent. Alternatively, a chiral nitrogen with one very bulky substituent (e.g., trityl) as in ligand **10** could give significant preference for one catalyst face over the other, because the coordinating oxygen apparently requires more room than the alkyl on the catalytic zinc. The bulkiest N-substituent has to interact with either the spectator alkyl or the substrate. Furthermore, if the ligand locks the bulkiest N-substituent in the pseudoaxial position in the catalyst complex, the interaction will be maximized (Figure 3). This is in effect what ligand **10** does. A more speculative conclusion is that one face of the catalyst could be blocked by a ligand with a bulky β-carbon substituent, which is locked in the more axial position when the catalyst

chelate ring is formed. Such a ligand should block the face of the catalyst with the axial β-carbon substituent quite well.

Blocking the syn-trans pathway seems to be best achieved by having a short chain linking the β-carbon and the nitrogen, as in ligands **8**, **9**, and **10**. However, it is crucial that the catalyst face with the bridge is the favored alternative for substrate and reagent coordination, for the bridge to block the syn-trans pathway. For ligand **7**, the 2-azabicyclo[2.2.1]heptyl moiety is so bulky that the catalyst face with the bridge is disfavored significantly. Clearly, blocking the syn-trans pathway requires a particular fine balance of the steric bulk on the favored catalyst face, because a too large bulk will either spoil selectivity induction or destroy catalytic activity altogether.

The anti-cis pathway is apparently automatically disfavored significantly for arylic aldehydes, but only disfavored slightly for simple aliphatic aldehydes. As there is essentially no difference between anti-trans and anti-cis pathways with respect to how much direct steric interaction the substrate and the ligand has, specific destabilization of the anti-cis pathway must be achieved by a different strategy. For example, placing a larger steric bulk on the catalytic zinc in lieu of the simple spectator alkyl would according to the model increase selectivity for aliphatic aldehydes.

Acknowledgment. We are grateful to the Danish Technical Sciences Research Council, the Danish Natural Sciences Research Council, and the Carlsberg Foundation for generous support. T.R. also wishes to thank Jeremy Greenwood and Jens Rudolph for many helpful discussions.

Supporting Information Available: The finalized MM3* parameters, an overview of the reference data set, all 17 B3LYP structures used for the force field parametrization, and the lowest-energy conformer for both the major and the minor enantiomer pathway for all 10 studied systems (PDF). This material is available free of charge via the Internet at http://pubs.acs.org.

JA0292952